THE STRANGE DENSITY OF MERCURY: THEORETICAL CONSIDERATIONS

A. G. W. CAMERON
Harvard-Smithsonian Center for Astrophysics

BRUCE FEGLEY, JR.
Massachusetts Institute of Technology

WILLY BENZ
Harvard-Smithsonian Center for Astrophysics
and

WAYNE L. SLATTERY
Los Alamos National Laboratory

Two classes of models which have been advanced to explain the high density of Mercury are reviewed and contrasted. These models invoke either the differing volatilities of iron and silicates or disruptive collisions to fractionate the two phases. We also contrast equilibrium condensation and planetary vaporization models, both of which fall within the first broad class considered. Our review indicates that equilibrium condensation models are unable to account for the observed high density of Mercury without invoking special mechanisms such as unrealistically narrow planetary accretion zones. However, we find that distinctive chemical differences, which are potentially testable by spacecraft experiments, provide means for distinguishing between planetary vaporization and large impact scenarios.

In *Mercury* (1988), M. S. Matthews, C. Chapman, and F. Vilas, Eds. University of Arizona Press, Tucson.

I. INTRODUCTION

Urey (1951,1952) first noted that the planet Mercury must have an iron to silicate ratio much larger than that for any other terrestrial planet because of its anomalously high density. The observed mean density of 5.44 g cm^{-3} (uncompressed ~5.3 g cm^{-3}) implies an iron to silicate mass ratio in the range from 66 : 34 to 70 : 30, about twice that of any of the other terrestrial planets, the Moon or the Eucrite Parent Body (Basaltic Volcanism Study Project 1981). The mean density of the Earth is 5.52 g cm^{-3}, corresponding to an uncompressed density of ~4.45 g cm^{-3} (Lewis 1972).

Three broad classes of models have been suggested to account for the anomalous composition of Mercury. One class of models employs scenarios which invoke differences in the physical properties (e.g., density, ferromagnetism, mechanical strength) of iron and silicates to achieve the required iron/silicate fractionation (Harris and Tozer 1967; Orowan 1969; Weidenschilling 1978; Smith 1979). A second class of models invokes the differing volatilities of iron and silicates to fractionate the two phases. Both equilibrium condensation (Lewis 1972) and vaporization (Bullen 1952; Ringwood 1966; Cameron 1985*a*) models are included within this class. A third class of models, relatively little explored so far, involves a scenario including major planetary collisions which are suggested to blow off the bulk of the silicate mantle from the original Mercury protoplanet (Smith 1979; Wetherill 1985*c;* Chapter by Wetherill).

In this chapter we shall ignore the first class of models and discuss the second and third classes. We shall have relatively little to say about the equilibrium condensation model because we find little evidence in its favor; indeed, our principal purpose here is to point out its shortcomings within the second class of models. We shall review at somewhat greater length the recent work by Cameron (1985*a*) and by Fegley and Cameron (1987) on the planetary vaporization model. We shall also report on the third class of planetary collision calculations carried out at Los Alamos by Benz, et al. (1986*a*,1987*b*).

There is an important distinction between the second and third classes of models. In the third class of models, physical fractionations of iron and silicates occur, and we would expect that Mercury would be composed of iron plus essentially chondritic silicates, with a diminution of the total mass; there would be little chemical fractionation, except to the degree that differentiation of the silicates (into crust and mantle) would remain apparent after physical fractionation. In the second class of vaporization models, volatility effects would lead to extensive chemical fractionations, and we would expect that the silicate phase in Mercury would undergo large compositional changes as a function of the extent of the postulated vaporization. This evolved composition would later be diluted by infalling planetesimals composed essentially of chondritic silicates. These compositional differences are an important means

of distinguishing between the proposed models and are potentially testable by a future Mercury mission.

II. THE EQUILIBRIUM CONDENSATION MODEL

In this early model (Lewis 1972), a very simple scenario was envisioned. The primitive solar nebula is supposed to be hot, isothermal at a given radius, and the accretion of the grains and the cooling of the nebula are assumed to be slow relative to gas-condensate reaction rates so that complete gas-solid equilibrium is attained. At pressures which conventional wisdom postulates for the nebula near the region of formation of Mercury (10^{-5} to 10^{-3} bar), metallic iron condenses at a slightly higher temperature than do the magnesium silicates. The theory seizes on this distinction between iron and silicates to postulate that this temperature gap can be responsible for the formation of an iron-rich planet.

Several authors have noted that this qualitatively appealing but unrealistically simple model is actually unable to account for the high uncompressed mean density of Mercury without recourse to such special mechanisms as aerodynamic sorting or to an unrealistically narrow accretion zone (Basaltic Volcanism Study Project 1981; Weidenschilling 1978; Lewis and Prinn 1984; Barshay 1981). The basic problem is that the condensation temperatures of Fe metal and of the magnesium silicates ($MgSiO_3$ and Mg_2SiO_4) are really so close together that it is extremely difficult to separate the two phases during accretion. This has stimulated the invention of special mechanisms for removal of silicate grains or for concentration of metal grains.

If condensation occurred under conditions more oxidizing than solar, as suggested by Mo and W depletions in many Ca-, Al-rich inclusions (Fegley and Palme 1985), then this problem is exacerbated because silicate condensation temperatures increase with increases in oxygen fugacity while that of Fe metal remains constant (Bartholomay and Larimer 1982; Palme and Fegley 1987).

On the other hand, if condensation occurred under conditions more reducing than solar which appears required for the enstatite chondrites (Larimer and Bartholomay 1979; Wasson's Chapter), then the silicate condensation temperatures decrease with a decrease in oxygen fugacity while that of Fe metal remains constant (Larimer and Bartholomay 1979). However, there are a number of problems with such a scenario. Large separations in the Fe metal and Mg_2SiO_4 condensation temperatures do not occur until the carbon/oxygen ratio is increased to about unity. No astrophysically reasonable mechanisms for changing the nebular C/O ratio from the solar value of 0.6 to the required value of unity have been proposed.

A further difficulty arises from the condensation of another suite of minerals including elemental carbon (graphite), SiC, CaS, MgS, AlN and TiN instead of ordinary silicates at C/O ratios above one. The large amount of

graphite ($\rho = 2.25$ g cm^{-3}) makes the production of a high density, iron-rich planet dependent upon having special mechanisms for separating the graphite from iron in the planet; there would be 2.5 times as much graphite (by mass) as Fe metal in the condensate. This problem might be avoided by assuming that condensation occurs at C/O ratios just below one where graphite will not form (Larimer and Bartholomay 1979). But in this case, the other unusual minerals still form in preference to ordinary silicates. There is no evidence from remote sensing for any such exotic mineralogy on the surface of Mercury, which resembles the lunar surface (Lewis and Prinn 1984, and references therein) with some differences (Chapter by Vilas). An additional point is that the mineral cohenite (Fe_3C) replaces Fe at a C/O ratio of unity. Cohenite is 2% less dense than Fe metal, so that it cannot be ruled out solely on this basis. Si-bearing Fe alloys may also form under reducing conditions (Lewis et al. 1979). However, these will lead to decreases in the density of the metal phase (e.g., the density of FeSi is 6.1 gm cm^{-3}, 22% less dense than Fe itself). It should be noted that equilibrium condensation under conditions sufficiently reducing to decrease significantly the silicate condensation temperatures (but not to produce graphite) predicts a volatile-rich Mercury containing about 12% of the solar carbon abundance, 4% of the solar nitrogen abundance, and 100% of the solar sulfur abundance. This is why we do not pursue this equilibrium model further.

III. PLANETARY VAPORIZATION

Cameron (1985*b*) has estimated that, during the evolution of the solar nebula, temperatures at the position of formation of Mercury were in the range of 2500 to 3500 K. Current studies of star formation in dense interstellar molecular clouds limit the time interval involved between the beginning of collapse and the turn-on of stellar luminosity to about 10^5 yr, in order that calculated evolutionary tracks in the HR diagram can fit observations of young clusters (Mercer-Smith et al. 1984). The high temperature region of the solar nebula near the radius of formation of Mercury may thus have been maintained for a time of the order of a few times 10^4 yr. The high temperatures indicated here are not subject to too much uncertainty, because that is the temperature range needed to radiate away the gravitational potential energy released when about one solar mass of gas is moved inside the orbit of Mercury (Cameron 1985*b*).

A protoplanetary form of Mercury can only have formed within the primitive solar nebula early enough to be exposed to these high temperatures in the nebula if gravitational instabilities occurred within the gas phase (forming giant gaseous protoplanets), and if small solid particles (clumps of interstellar grains from which ices have evaporated) were able to settle within the gaseous protoplanets to form very refractory bodies. Such gaseous protoplanets can only form in the nebula very early, before much mass has had a chance to

collect at the center of the disk. They are very large and quite cool, and the gas is expected to evaporate quite soon after formation as the temperature in the nebula increases (Cameron et al. 1982). This would leave a condensed protoplanet. Cameron has assumed that the original Mercury protoplanet, if close to a chondritic silicate/iron ratio, would be about 2.25 times the mass of the present Mercury.

The nebula surrounding any such early proto-Mercury would be optically thick (Cameron 1985*b*). Within the relevant time scale, the blackbody radiative energy input to the planet is much more than sufficient to vaporize the entire mantle (Cameron 1985*a*). The protoplanet would also be situated in a strong solar nebula wind, composed of both a fixed and a fluctuating component, with a velocity relative to the protoplanet of the order of 1 km s^{-1}. The fixed component arises from the fact that the gas is partially supported in the radial direction by a pressure gradient, whereas the protoplanet is not; thus, there are two different orbital velocities needed for the centripetal support of the gas and the protoplanet. The fluctuating component comes from the turbulent velocity expected to be present within the disk and responsible for the turbulent viscosity that dissipates the disk on such a short time scale. It is this same turbulence that prevents gravitational instabilities from occurring either in the gaseous or the solid components of the nebula during the strongest part of the dissipation. Cameron has suggested that this wind may be able to carry away most of the vaporized mantle of the planet, although the process only marginally satisfies the energy requirements.

The physical scenario is as follows. Inflowing radiant energy heats the surface rocks of the protoplanet and increases the rate of vaporization of the rocky constituents. The resulting vapors accumulate until the surface pressure of the resulting atmosphere reaches the value that corresponds to chemical equilibrium; actually this phase would be quickly achieved so that the condition for chemical equilibrium can be assumed for the entire period. It is this atmosphere which forms the interface between proto-Mercury and the nebular wind. In Cameron's models the surface pressure of the rock vapor products is some two orders of magnitude greater than the pressure in the surrounding solar nebula; thus, solar nebula hydrogen can reach the planetary surface only by forced downward turbulent mixing, which is very inefficient in the face of continued removal of the rock vapor atmosphere by the wind and the continued renewal of the atmosphere by vaporization at its base.

The energy required for removal of the rock vapor atmosphere can reside only in the kinetic energy of the nebula wind. The wind will force turbulent mixing of the outer layers of the rock vapor atmosphere and the solar nebula. The effective scale height of the planetary atmosphere will be increased as the mean molecular weight decreases by such mixing. This process will continue to increase the height of the planetary atmosphere until the turbulent flow of the solar nebula wind past the protoplanet is able to entrain parcels of the atmosphere and carry them away. Cameron has estimated that this interface

will exist at an effective planetary atmosphere radius of about three times the radius of the planet, where the kinetic energy of the nebula wind impacting the protoplanet is an order of magnitude greater than the energy required to remove the vaporized mantle to infinity in about 3×10^4 yr. Thus, the operation of this scheme requires that the kinetic energy of the wind be used for this purpose with about 10% efficiency. It is not known whether this is possible.

The temperature range 2500 to 3500 K is above the liquidus temperatures (at 1 bar) of chondritic silicates and refractory mineral assemblages in Ca,Al-rich inclusions, so at least the surface layers would be molten. Furthermore, the postulated scenario requires proto-Mercury to be formed very hot, and hence we make the reasonable assumption that the entire silicate phase of proto-Mercury would be a silicate magma. The calculations in Cameron (1985*a*) were based on the vaporization of a silicate magma with the composition $MgSiO_3$ and did not attempt to examine the vaporization chemistry of more complex silicate materials. That task was carried out by Fegley and Cameron (1987).

Fegley and Cameron (1987) report the results of a series of calculations to study the compositional evolution of a silicate magma (with initial composition being approximately chondritic) as a function of the extent of vaporization. The composition of a totally molten silicate magma and of the vapor phase in equilibrium with it was calculated using a multicomponent gas-melt chemical equilibrium code based on the silicate melt solution models developed by Hastie and coworkers (1982*a*,*b*,1984,1985). The calculations were done as a function of the degree of vaporization at 2500 to 3500 K. Both ideal and nonideal magma solution models were studied.

The initial composition of the magma was assumed to be a mixture of the oxides SiO_2-MgO-CaO-Al_2O_3-TiO_2-Na_2O-K_2O-FeO-UO_2-ThO_2-PuO_2 in relative solar proportions (Anders and Ebihara 1982) except for FeO which was set to 0.1 times the MgO abundance. The remainder of the Fe solar abundance was assumed to form the core of proto-Mercury. The actinides and K were included in the calculations to study the effect of vaporization on the amounts of heat-producing radionuclides left in the planet after partial vaporization. Inclusion of the alkalis also provides a comparison with Hastie's work. The use of a more refractory starting composition would not significantly affect the results of these calculations. In fact, such compositions appear as intermediate stages during the vaporization process.

The calculated compositions were for the equilibrium between the gas and melt phases. Thermodynamic data were obtained from standard sources (Stull and Prophet 1971; Chase et al. 1971–1975, Glushko et al. 1978–1982) as well as elsewhere in the literature (see Fegley and Cameron 1986 for detailed references). An ideal magma was considered to be one in which the activity coefficients of the constituent oxides were taken to be unity. In a nonideal magma these coefficients were usually orders of magnitude smaller; the procedure of Hastie and his coworkers assumes that the magma is com-

posed of a large number of pseudospecies, so that the abundances of the basic oxides, which are included among the pseudospecies, are greatly reduced, along with the corresponding activities. The vaporization calculations agreed well with experimental results of Hashimoto (1983), giving some confidence in the method.

Results of the vaporization calculations for the composition of the proto-Mercury mantle in the ideal solution case at 3000 K are shown in Fig. 1. The first elements lost during vaporization are the alkalis, Na and K, with K being more volatile. The next element lost is Si, followed by Fe and Mg. At the highest degree of vaporization (~4.6% residual mantle mass fraction), ~95% of the Al, ~40% of the Ca and ~15% of the Ti remain in the mantle.

Figure 2 shows the results for the vaporization of the mantle in the non-ideal solution case, also at 3000 K. Several interesting features are displayed. The alkalis are still the most volatile elements but Fe is the next element lost, followed by Si and Mg. However, Mg loss from the magma accelerates after about 80% of the silicate has been vaporized. At the highest degree of vaporization considered (96% of original silicate lost), more Si remains in the magma than Mg. Loss of Ca and Ti is also occurring at this point. More Ti (53%) but less Ca (33%) remain in the magma relative to the ideal magma case.

The calculated mantle density for these cases is shown in Fig. 3. The ideal solution case is shown as the dashed line; it has a complicated structure. The density increases to a maximum at 3.71 g cm^{-3} when approximately 28% of the original silicate remains. The mantle density then decreases with

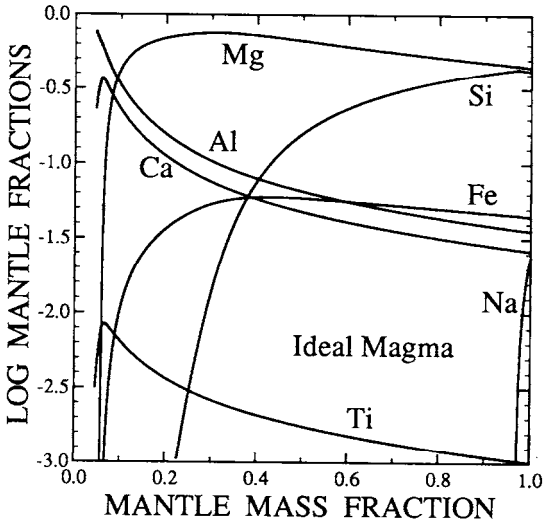

Fig. 1. The composition of the mantle as a function of its remaining mass fraction as vaporization proceeds, for an ideal magma. The elements shown are balanced by oxygen in the mantle. K is not shown because it coincides with the right frame starting close to the bottom.

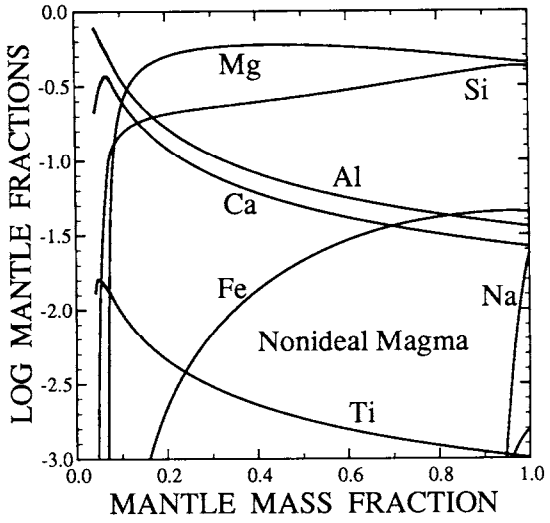

Fig. 2. The composition of the mantle as a function of its remaining mass fraction as vaporization proceeds, for a nonideal magma. The elements shown are balanced by oxygen in the mantle. The unlabeled line in the lower right corner is potassium.

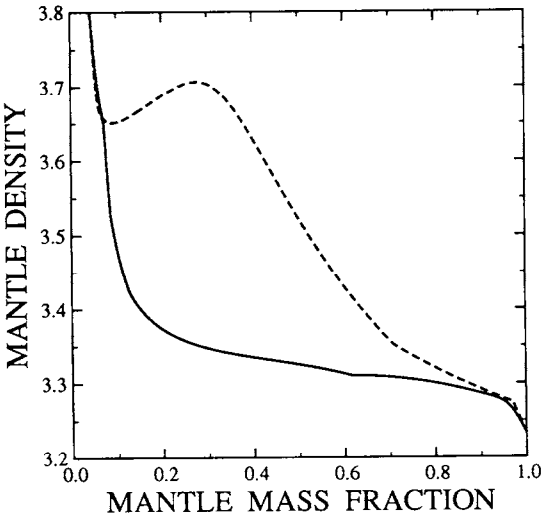

Fig. 3. The density of the mantle as a function of the remaining mantle mass fraction as vaporization proceeds. The dashed line is for an ideal magma; the solid line is for a nonideal magma, both at 3000 K.

increasing vaporization until about 10% of the silicate remains and the density is about 3.65 g cm^{-3}. The density then starts increasing again with further vaporization and is virtually indistinguishable from the density profile for the nonideal magma case, shown as the solid line. However, in the nonideal case there is a marked difference in the behavior of the density in the earlier stages of the vaporization. After quickly rising to about 3.3 g cm^{-3} as the alkalis are lost, the density then stays at nearly the same value until almost 80% of the mass has been lost. Further vaporization then causes a rapid rise in the density.

The calculated mean uncompressed density of the planet, shown in Fig. 4 for the ideal (dashed-line) and nonideal (solid-line) cases, monotonically increases with the degree of vaporization in each case. The uncompressed mean density of 5.3 g cm^{-3} for Mercury is reached after about 72% (ideal) to 79% (nonideal) of the mantle has been vaporized. The calculated composition of the silicate phase at this point is given in Table I, which also includes the results of nonideal calculations for temperatures of 2500 K and 3500 K. The (possible) later accretion of ordinary silicate (MgO-, SiO_2-rich) planetesimals would change these compositions by adding more SiO_2, FeO and alkalis. However, the observed mean density of the planet could then be obtained only if more than 72% to 79% of the mantle had originally been vaporized and lost, leaving the remaining fraction of the original mantle even more refractory.

The heat-producing radionuclides behave in two quite different fashions during vaporization. Loss of K occurs early during the vaporization process. U is also lost during vaporization and is depleted much more than Pu (approx-

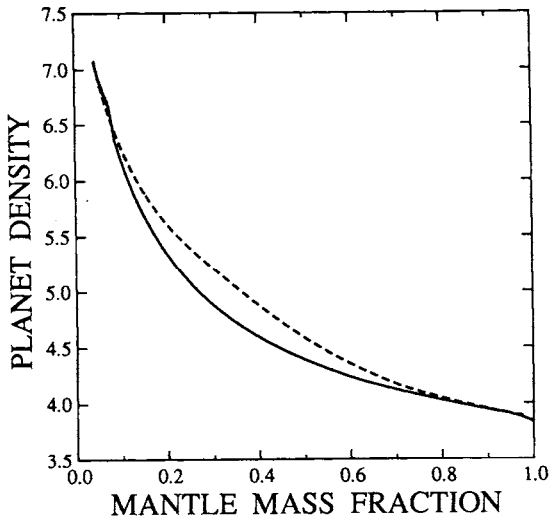

Fig. 4. The density of the Mercury protoplanet as a function of the remaining mantle mass fraction as vaporization proceeds. The dashed line corresponds to an ideal magma; the solid line is for a nonideal magma, both at 3000 K.

TABLE I
Predicted Mantle and Crust Compositions from Different Vaporization Models[a]

Oxide	Mass % Oxide in Different Models[c]			
Model	1	2	3	4
SiO_2	1.2	32.1	25.9	19.9
CaO	9.9	14.6	13.7	11.7
MgO	67.7	34.5	42.3	50.0
Al_2O_3	12.4	18.1	17.0	14.4
FeO	8.3	0.0	0.4	3.4
TiO_2	0.5	0.7	0.8	0.6
K(ppb)	0.0	0.0	0.0	0.0
U(ppb)[b]	0.0	0.0	0.0	0.3
Th(ppb)[b]	278	401	377	322

[a]Mean uncompressed density = 5.3 g cm^{-2}.
[b]Primordial abundances 4.55 × 10^9 yr ago.
[c]Models: 1. Ideal magma, 3000 K; 2. Nonideal magma, 2500 K; 3. Nonideal magma, 3000 K; 4. Nonideal magma, 3500 K.

imately as volatile) or Th (less volatile). This is due to the formation of volatile U-oxide gases. In contrast, Pu and Th are essentially undepleted by vaporization by the time that the mean uncompressed planetary density of 5.3 g cm^{-3} is reached.

In each case in Table I, the calculated mean uncompressed planetary density is 5.3 g cm^{-3}, which matches the value deduced for Mercury. All four compositions in the table are depleted in the alkalis, FeO and SiO_2, and are enriched in CaO, MgO, Al_2O_3 and TiO_2 relative to chondritic material. There is a large difference, which brackets the end-member compositions expected from vaporization of a silicate magma, between the results of the ideal and nonideal models. Further discussion centers on the latter models because of the good agreement of these runs with the available data on silicate vaporization and activity coefficients.

The uncompressed planetary mean density was matched with a metal-to-silicate mass ratio of approximately 64 to 36, with the silicate phase considerably reduced in SiO_2 relative to some of the metal oxides. Inclusion of Ni in the metal phase will decrease slightly the calculated metal abundance because Ni is denser than Fe (8.90 vs 7.86 g cm^{-3}, respectively). However, this is a second-order effect; an alloy with the solar Ni abundance and Fe decreased by forming FeO = 0.1 MgO (as in our models) is only 0.8% denser than pure Fe.

The silicate phase is predicted to be depleted in the alkalis, FeO and SiO_2 and enriched in CaO, MgO, Al_2O_3 and TiO_2 relative to chondritic material. The vaporization models also predict that the silicate is depleted in SiO_2 and enriched in other oxides (CaO, MgO, Al_2O_3, TiO_2 and FeO) relative to sili-

cate compositions calculated for equilibrium condensation models of Mercury (Basaltic Volcanism Study Project 1981). Another prediction of the vaporization models calculated by Fegley and Cameron (1987) is the production of trace-element abundance patterns which are depleted in easily oxidized elements relative to other refractory trace elements of similar volatilities. In particular, the depletion of U, Ce and other easily oxidized rare earth elements is expected. These abundance patterns are unique signatures due to vaporization and are not produced in other models (e.g., equilibrium condensation). These differences will influence several aspects of Mercury's composition and structure including: (a) the mineralogy of the silicate phase; (b) the nature of a crust (if a distinct, differentiated crust exists); (c) the chemical composition and physical properties, such as viscosity, of volcanic magmas; and (d) trace element partitioning between putative magmas and their source regions.

IV. PLANETARY COLLISIONS

The scenario in which a major planetary collision may have played a role in producing the strange density of Mercury is that of planetary accumulation from planetesimals. It is assumed that the primitive solar nebula has largely dissipated with the formation of the Sun, during which time it is highly turbulent and produces dissipation via a large turbulent viscosity (Cameron 1985*b*). After the turbulence dies away, small solid bodies, presumably in the form of clumps of interstellar grains, are able to settle to midplane, where they are likely to become gravitationally unstable to the formation of planetesimals of small asteroidal size (a few kilometers in radius) (Goldreich and Ward 1973). There follows an accumulation of these planetesimals into bodies of increasing size (Wetherill 1980*a*). This accumulation tends to produce a largest body in a given feeding zone, with the next largest body less in mass by a factor of a few, and so on down from there. The term feeding zone is inexact, since the source material for the accumulation of any one of the terrestrial planets is actually spread over the inner solar system. We use it here to refer to the volume of space dominated by the final accumulated planet.

Toward the end of the accumulation process the second largest body is likely to collide with the largest, with potentially surviving observable effects. In the case of the Earth this is the collision that may have initiated the formation of the Moon (Hartmann and Davis 1975; Cameron and Ward 1976; Benz, et al. 1986). In fact, more recent calculations (Benz et al. 1987*b*) have narrowed down the set of acceptable parameters to a collision between the proto-Earth and a body of 0.13 to 0.17 times its mass, taking place at rather low velocity. For the case of Mercury we have carried out similar collisional calculations. We have assumed that the target protoplanet Mercury was 2.25 times the mass of the present Mercury, in order to give it approximately a chondritic silicate to iron ratio, and we have hit it with a projectile of one-sixth that mass at somewhat higher velocities.

These calculations have required the use of a 3-dimensional hydrodynamic code run on Cray computers at Los Alamos. The method used is called "smoothed particle hydrodynamics," and has been described by Benz et al. (1986*a*). Briefly, the mass distribution in the target and the projectile is represented by mass points distributed in proportion to the density; these mass points are actually considered to have a finite distribution in space as defined by the shape of their "kernels". In condensed matter these kernels overlap, and one obtains bulk properties like pressure and density by a suitable averaging over the mass points. In Benz et al. (1986*a*) the kernels were given an exponential shape, but here they were given a polynomial form because the resulting sharp cutoff in the spatial distribution made the calculations easier.

Also described in Benz et al. (1986) was the Tillotson equation of state that was used in the earlier calculations of the proto-Mercury collisions. With this equation of state, rocky material was represented by granite, for which the relevant data were available at Los Alamos. Beyond our Mercury run 7, the ANEOS equation of state was used which was developed at the Sandia Laboratories (Thompson and Lauson 1984). This equation of state has a better representation of mixed phase conditions, when both a vapor phase and a condensed matter phase are present at the same time. For rocky material we used dunite with this equation of state; the appropriate equation of state parameters for this material were determined by J. Melosh, and we are grateful to him for providing them to us.

For our earliest proto-Mercury collision runs we used a relatively small number of particles; these results were for our preliminary orientation to the problem, and we do not report them here. These early runs used rock plus an iron core for the target but just rock for the projectile. After run 4, the projectile had an iron core as well. In these runs the proto-Mercury target was represented by 3000 particles, of which 959 were iron and 2041 were silicate rock. The projectile of one-sixth the mass was represented by 1000 particles, each half the mass of the particles used in the target. In the projectile, 319 of the particles were iron (beyond run 4) and 681 were rock.

The results of the collision calculations are shown in Table II. In runs 3 and 4 we were still getting our bearings, and the projectile was made entirely of rock. In run 3 the projectile had an impact velocity of 27 km s^{-1} at infinity; it hit the target centrally and knocked off most of the silicate rock and some of the iron. This would be a very good candidate for the kind of collision that would produce the observed Mercury in this scenario, except that the composition of the projectile is unrealistic. In run 4 the velocity of the impactor was increased to 38 km s^{-1}, resulting in the complete disruption of the target.

With run 5, we started a realistic series of cases by putting an iron core into the projectile. We chose an impact velocity of 25 km s^{-1} and found that the target was once again totally disintegrated. It was thus evident that the denser core in this impactor enabled the target to be disintegrated at a significantly lower velocity than was true of the softer case in which the impactor

TABLE II
The Outcome of the Mercury Collision Scenarios

Case	Vel. km/sec	Impact Param.[a]	Targ. Iron[b]	Proj. Iron[b]	Targ. Sil.[b]	Proj. Sil.[b]	Sil./Iron Ratio	Mass Ratio[c]
3	27	0.00	76.5%		5.1%	0.4%	0.14	0.67
4	38	0.00			Disintegrated			
		Below here the impactor had an iron core						
5	25	0.00			Disintegrated			
6	20	0.00	56.1%	37.7%	5.9%	7.5%	0.25	0.58
7	22	0.46	93.1%	7.2%	22.0%	2.8%	0.51	1.18
		Below here the ANEOS equation of state was used						
8	20	0.00	48.8%	42.0%	8.8%	11.3%	0.41	0.60
9	15	0.00	86.2%	69.3%	42.1%	31.3%	1.03	1.67
10	10	0.00	99.2%	97.8%	79.1%	58.6%	1.64	2.65
11	15	0.59	99.4%	0.6%	70.3%	12.3%	1.55	2.33
12	20	0.51	94.3%	3.8%	47.1%	6.8%	1.08	1.76
13	28	0.53	80.0%	0.0%	20.0%	1.2%	0.54	1.03
14	35	0.54	57.0%	0.3%	7.8%	0.3%	0.29	0.59

[a]The impact parameter is given in units of the target radius.
[b]The values given for target and projectile iron and silicate are the percentages of the numbers of particles in the residual body coming from these four sources.
[c]The mass ratio is the residual mass relative to the present mass of the planet Mercury (3.3×10^{26} gm).

was just rock. In run 6 the velocity was lowered to 20 km s^{-1} and the target survived the collision, after once again losing nearly all its silicates. It is interesting to note, however, that the iron core in the target lost 43.9% of its mass but picked up 37.7% of the mass of the iron core in the projectile. This is an excellent candidate to be the scenario for the formation of Mercury. However, in run 7, with an impact velocity raised slightly to 22 km s^{-1} and an impact parameter of nearly half the planetary radius, the collision leaves more than the present mass of Mercury, and hence this is not a good candidate for the Mercury scenario, especially since some of the lost mass will be reaccumulated, as discussed below.

Starting with run 8, we used the ANEOS equation of state. Run 8 was essentially a repeat of the conditions in run 6. The results of these two runs were very similar, showing that the results do not depend sensitively on the character of the equation of state and the choice of rocky material. The amount of iron left in the residual body is nearly the same; there is a little less iron from the target and a little more from the projectile. The total mass left behind after the collision is nearly the same in the two cases, and is a satisfactory value of only about 60% of the present mass of Mercury.

Runs 9 and 10 were head-on collisions like run 8, but at progressively lower collision velocities, 15 km s^{-1} for run 9 and 10 km s^{-1} for run 10. The amount of mass ejected in the collision decreases with decreasing collision

velocity, so that in the 10 km s^{-1} case the planet is left with more mass than it had at the beginning. Neither of these cases is a candidate to produce the current Mercury.

Runs 11 and above were further cases in which the projectile hit the target off-center, with impact parameters just over half the radius of the target. The striking characteristic of these runs is that such off-center collisions are much less effective in ejecting mass from the target. Whereas a central collision at 20 km s^{-1} leaves only 0.60 Mercury masses, a similar collision which is noncentral leaves 1.76 Mercury masses, too high to make this a candidate collision for the present Mercury. Only in run 14, where the impact velocity was 35 km s^{-1}, does the planetary remnant become reduced to 0.59 Mercury masses, which makes it a good candidate for forming the observed planet.

As discussed in the introduction, the present silicate/iron ratio in Mercury is about in the range 0.4 to 0.5, and this should be regarded as equal to or more than the value to be expected in the remnant produced in these calculations for the result to be considered a candidate collision to lead to the present Mercury. The only cases (see Table II) which satisfy this criterion and which result in nearly complete silicate loss and relatively little net iron loss from proto-Mercury is a nearly central collision at about 20 km s^{-1} and a noncentral collision at about 35 km s^{-1}. The amount of mass lost is a sensitive function of the collision velocity and the impact parameter.

In the course of a typical collision, a great deal of material is thrown out from the site of the collision, some to escape and the rest to fall back onto the planet. Of the material thrown out, much is clumped into clusters of particles and the rest consists of single particles. These "single particles" are likely to have passed through the vapor phase and many of them will have recondensed with expansion of the material. At the end of the Cray runs this is the typical situation: a cloud of material surrounding a planetary core, some of it rising and the rest falling back. From our post-Cray analyses of the results, we find that nearly all of the larger clumps of particles (which tend to be iron-rich) fall back onto the planet and nearly all of the single particles escape. In the cases where the planet is disintegrated, this clumpy situation still exists, but the largest clumps are only of moderate size and very few of them collide with one another.

In a central collision at about 20 km s^{-1} a striking pattern develops in the debris. The planetary core is deformed into a relatively thin sheet, and the material which is thrown out is largely ejected in essentially the same thin sheet (the silicate is somewhat more dispersed than the iron). Figure 5 shows a plot of the debris at the end of the Cray run 8, viewed from a direction at right angles to the direction of collision, which shows the sheet. Figure 6 is a plot of the same case but viewed from the direction of the collision. In these plots the open circles are silicate particles and the filled circles are iron particles; the silicate particles do not hide other particles beyond them, so that the iron particles are fully visible.

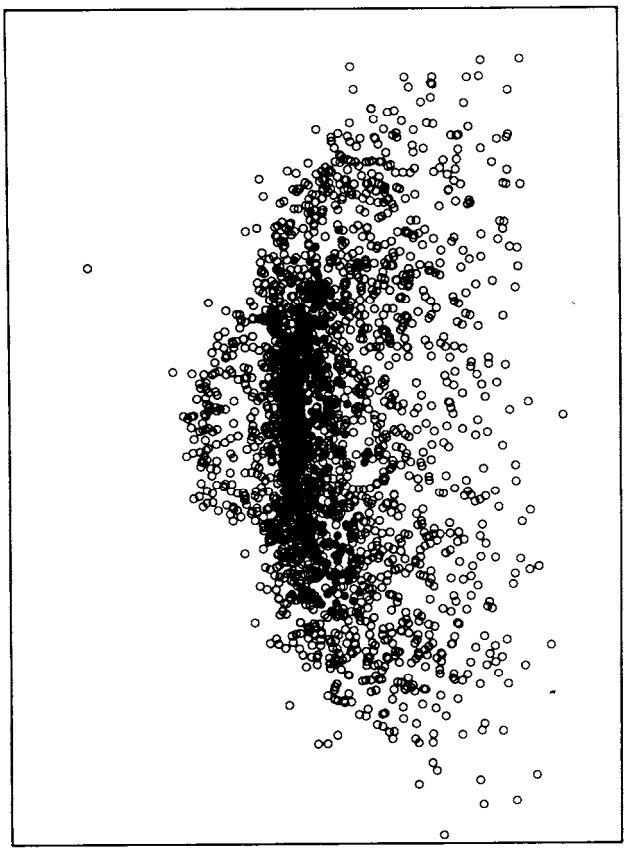

Fig. 5. A plot of the positions of the silicate (open circles) and iron (filled circles) particles at the end of Cray run 8, viewed along a right angle to the line of collision.

It is evident that a successful collision should be judged to be one in which the mass of the protoplanet is reduced well below that of the present planet Mercury and in which the remnant is composed predominantly of iron. All of the material which is ejected in the collision goes into independent orbit around the Sun; these orbits must necessarily cross the orbit of the remaining protoplanet. The present orbital elements of Mercury are subject to secular variation with time due to other planetary perturbations, so we do not know what the orbit of the remnant would have been. Nevertheless, we took the present orbit of Mercury as a suitable prototype of that orbit, and calculated whether any of the particles ejected from the collision would have been put into orbits that would cross the orbit of Venus. We found that, in general, only a few of the particles would do so if ejected at aphelion, and usually a few dozen and at most a few hundred would do so at perihelion. Thus, only a

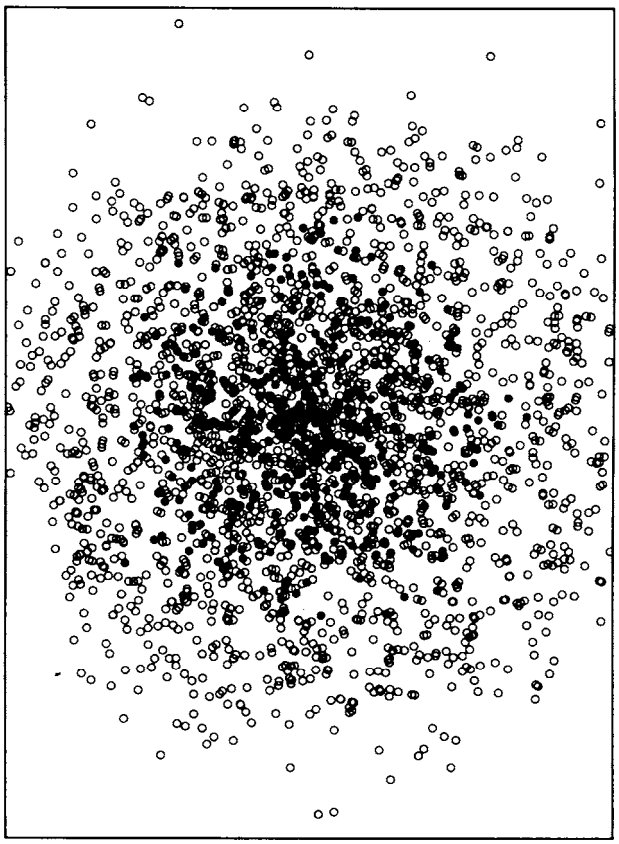

Fig. 6. A plot of the positions of the silicate (open circles) and iron (filled circles) particles at the end of Cray run 8, viewed along the direction of collision.

minority of the particles can be removed from Mercury-crossing orbits by other planetary perturbations.

The key to the question of whether the particles are reaccreted by Mercury probably lies in the fact that most of the ejected material has passed through the vapor phase. Upon expansion, this material will cool and condense into solid particles, but if the vapor is by that time at fairly low density, then the particle sizes will probably be very small, in the subcentimeter size range. Such small particles will be drawn into the Sun by the Poynting-Robertson effect in a time short compared to their expected collision time with Mercury, which is about 10^6 yr (G. Wetherill, personal communication). If a substantial part of the ejected material has sizes in the centimeter range, then the individual pieces would undergo a large number of collisions with one another, tending to grind themselves down to a size that can be removed by the Poyn-

ting-Robertson effect. Very much larger chunks ejected from the collision may not be ground down enough for Poynting-Robertson removal, and these are likely to be reaccumulated upon Mercury.

Thus, this scenario appears promising to account for the strange density of Mercury.

V. DISCUSSION

In this chapter we have discussed three scenarios which have been postulated to account for the high mean density of Mercury. We found little of merit in the equilibrium condensation scenario. We have found the planetary evaporation scenario to lead to some interesting predictions about the chemical composition of the present Mercury mantle. The efficiency of the postulated wind mechanism for the removal of the evaporated rock decomposition products from proto-Mercury is uncertain. A major planetary collision is a plausible occurrence in the late stages of planetary accumulation, and we have found that reasonable circumstances exist in which most of the silicates can be stripped from the protoplanet. We are uncertain about the amount of reaccumulation of these silicates that will take place from orbit. The chemical differences predicted between the second and third scenarios may provide a means for distinguishing between these scenarios observationally by means of spacecraft experiments.

Acknowledgments. This research has been supported in part by the National Aeronautics and Space Administration to Harvard University and to Massachusetts Institute of Technology. W. Benz also acknowledges support from the Swiss National Science Foundation. We are grateful to the Los Alamos National Laboratory for the provision of the computer time which has been used on this problem.